

## DETECTION OF ATOMIC CARBON [C II] 158 $\mu$ m AND DUST EMISSION FROM A $Z = 7.1$ QUASAR HOST GALAXY

B. P. VENEMANS

Max-Planck Institute for Astronomy, Königstuhl 17, 69117 Heidelberg, Germany and  
European Southern Observatory, Karl-Schwarzschild Strasse 2, 85748 Garching bei München, Germany

R. G. MCMAHON

Institute of Astronomy, University of Cambridge, Madingley Road, Cambridge CB3 0HA, UK and  
Kavli Institute for Cosmology, University of Cambridge, Madingley Road, Cambridge CB3 0HA, UK

F. WALTER AND R. DECARLI

Max-Planck Institute for Astronomy, Königstuhl 17, 69117 Heidelberg, Germany

P. COX AND R. NERI

Institut de Radioastronomie Millimetrique, 300 rue de la Piscine, 38406 Saint Martin d'Herès, France

P. HEWETT

Institute of Astronomy, University of Cambridge, Madingley Road, Cambridge CB3 0HA, UK

D. J. MORTLOCK

Astrophysics Group, Imperial College London, Blackett Laboratory, Prince Consort Road, London, SW7 2AZ, UK and  
Department of Mathematics, Imperial College London, London, SW7 2AZ, UK

C. SIMPSON

Astrophysics Research Institute, Liverpool John Moores University, Twelve Quays House, Egerton Wharf, Birkenhead, CH41 1LD, UK

AND

S. J. WARREN

Astrophysics Group, Imperial College London, Blackett Laboratory, Prince Consort Road, London, SW7 2AZ, UK  
*The Astrophysical Journal Letters, 751:L25 (5pp), 2012 June 1*

### ABSTRACT

Using the IRAM Plateau de Bure Interferometer, we report the detection of the 158  $\mu$ m [C II] emission line and underlying dust continuum in the host galaxy of the quasar ULAS J112001.48+064124.3 (hereafter J1120+0641) at  $z = 7.0842 \pm 0.0004$ . This is the highest redshift detection of the [C II] line to date, and allows us to put the first constraints on the physical properties of the host galaxy of J1120+0641. The [C II] line luminosity is  $1.2 \pm 0.2 \times 10^9 L_{\odot}$ , which is a factor  $\sim 4$  lower than observed in a luminous quasar at  $z = 6.42$  (SDSS J1148+5251). The underlying far-infrared (FIR) continuum has a flux density of  $0.61 \pm 0.16$  mJy, similar to the average flux density of  $z \sim 6$  quasars that were not individually detected in the rest-frame FIR. Assuming that the FIR luminosity of  $L_{\text{FIR}} = 5.8 \times 10^{11} - 1.8 \times 10^{12} L_{\odot}$  is mainly powered by star formation, we derive a star formation rate in the range  $160 - 440 M_{\odot} \text{ yr}^{-1}$  and a total dust mass in the host galaxy of  $6.7 \times 10^7 - 5.7 \times 10^8 M_{\odot}$  (both numbers have significant uncertainties given the unknown nature of dust at these redshifts). The [C II] line width of  $\sigma_V = 100 \pm 15 \text{ km s}^{-1}$  is among the smallest observed when compared to the molecular line widths detected in  $z \sim 6$  quasars. Both the [C II] and dust continuum emission are spatially unresolved at the current angular resolution of  $2.0 \times 1.7 \text{ arcsec}^2$  (corresponding to  $10 \times 9 \text{ kpc}^2$  at the redshift of J1120+0641).

*Subject headings:* cosmology: observations — galaxies: active — galaxies: high-redshift — galaxies: individual (ULAS J112001.48+064124.3) — galaxies:ISM

### 1. INTRODUCTION

Understanding the formation of the earliest quasars and host galaxies has become of great importance since the discovery of the bulge mass–black hole mass cor-

relation in nearby galaxies, a result which led to the suggestion of a fundamental relationship between (massive) black holes and spheroidal galaxy formation (e.g. Tremaine et al. 2002; Marconi & Hunt 2003). So far, the stellar component of the host galaxies of luminous  $z \simeq 6$  quasars have defied detection at (observed) optical and

near-infrared wavelengths, which is typically attributed to the central point sources outshining their surroundings. On the other hand, observations of the molecular gas, through emission lines of, e.g., CO, redshifted in the millimeter and radio wavebands allows one to probe the total gas mass and derive the dynamical mass of the high redshift quasar hosts. These observations indicate that the high- $z$  quasars are associated with active star forming host galaxies with star formation rates (SFRs)  $\sim 1000 M_{\odot} \text{ yr}^{-1}$  (Wang et al. 2008).

The  $\text{C}^+$  fine structure line at  $157.74 \mu\text{m}$  (hereafter [C II]  $158 \mu\text{m}$ ) is one of the strongest cooling lines in the warm interstellar medium (ISM), containing up to 1% of the far-infrared (FIR) emission in local starburst galaxies (Stacey et al. 1991). COBE observations of the Milky Way (Wright et al. 1991) show that this transition is the strongest FIR line emitted by the ISM in our Galaxy ( $L_{[\text{CII}]} = 5 \times 10^7 L_{\odot}$ ). For sources at redshifts  $z \gtrsim 4$ , the [C II] emission line is redshifted to the sub/millimeter and becomes observable using ground based facilities. Early attempts to detect the [C II] line in the  $z = 4.7$  quasar BR1202–0725 by Isaak et al. (1994) were unsuccessful due to technological limitations. More recently, [C II] has been detected in a number of  $z > 4$  quasar host galaxies and submillimeter galaxies, including BRI 0952–0115 ( $z = 4.43$ ; Maiolino et al. 2009), BRI 1335–0417 ( $z = 4.41$ ; Wagg et al. 2010), LESS J033229.4 ( $z = 4.76$ ; De Breuck et al. 2011) and SDSS J1148+5251 ( $z = 6.42$ ; Maiolino et al. 2005).

To further constrain the build-up of massive galaxies at the earliest cosmic epochs, it is imperative to locate and study bright quasars at the highest redshifts possible. Recently, Mortlock et al. (2011) discovered a bright quasar at a redshift  $z = 7.085$ , ULAS J112001.48+064124.3 (hereafter J1120+0641), the only quasar currently known at  $z > 7$ . The absolute magnitude of  $M_{1450} = -26.6$ , the black hole mass of  $2.0_{-0.7}^{+1.5} \times 10^9 M_{\odot}$  and (metal) emission line strengths (Mortlock et al. 2011) are all comparable to those observed in  $z \simeq 6$  quasars. Here we present the detection of the redshifted [C II]  $158 \mu\text{m}$  emission line and the underlying dust far-infrared continuum emission in J1120+0641. In Section 2 we introduce the observations obtained with the IRAM Plateau de Bure Interferometer (PdBI), followed by a description of our results in Section 3. In Section 4 we discuss the implications of our findings and we present a summary in Section 5. Throughout this Letter a concordance cosmology with  $H_0 = 70 \text{ km s}^{-1} \text{ Mpc}^{-1}$ ,  $\Omega_M = 0.3$  and  $\Omega_{\Lambda} = 0.7$  is adopted, leading to a luminosity distance for a source at  $z = 7.085$  of  $D_L = 70.0 \text{ Gpc}$ , a spatial scale of  $5.2 \text{ kpc arcsec}^{-1}$ . The age of the universe at  $z = 7.085$  is  $740 \text{ Myr}$ .

## 2. OBSERVATIONS

Observations of the [C II]  $157.74 \mu\text{m}$  ( $\nu_{\text{rest}} = 1900.54 \text{ GHz}$ ) line in J1120+0641 at a redshift  $z = 7.085$  (observed frequency of  $235.07 \text{ GHz}$ , or  $1.276 \text{ mm}$ ) were carried out between 2011 March and 2012 January with the WideX correlator using the PdBI. The quasar was observed on 2011 March 9 for 2.9 hr with five antennas in C configuration, and on 2011 December 13 and 15 and 2012 January 12 and 18 for a total of 6.3 hr with six antennas

in D configuration. For the phase calibration the source J1055+018 was observed every 30 minutes. Absolute flux calibration was obtained by observing 3C273 and MWC349 before and after each track. The WideX correlator provides an instantaneous bandwidth of  $3.6 \text{ GHz}$  in dual polarization, which corresponds to  $\sim 4400 \text{ km s}^{-1}$  at  $235 \text{ GHz}$ . With the goal to have a better measurement of the continuum level, the frequency setup was shifted by  $+1000 \text{ km s}^{-1}$  after the 2011 March observations. The total on-source integration time was  $8.25 \text{ hr}$  (six antenna equivalent).

The data were reduced using the Grenoble Image and Line Data Analysis System (GILDAS) software<sup>1</sup>. The data were rebinned to a resolution of  $20 \text{ MHz}$  ( $25.5 \text{ km s}^{-1}$ ). The final resolution of the image where both frequency setups overlap is  $2''.02 \times 1''.71$  at a position angle of  $23^\circ$ . The rms of the final image is  $\sim 1.09 \text{ mJy beam}^{-1}$  per  $20 \text{ MHz}$  bin.

## 3. RESULTS

The final spectrum of the [C II] emission line and the underlying continuum towards J1120+0641 is shown in Figure 1 (top panel). The [C II] emission is clearly detected at a redshift of  $z = 7.0842 \pm 0.0004$ . This is slightly blueshifted (by  $-30 \pm 14 \text{ km s}^{-1}$ ) but consistent with the redshift of  $z = 7.085$  (Mortlock et al. 2011), which was derived by fitting the template of Hewett & Wild (2010) to the rest-frame UV emission lines. The [C II] emission line has a peak flux density of  $f_P = 4.12 \pm 0.51 \text{ mJy beam}^{-1}$ . In addition, the underlying (rest-frame) far-infrared continuum is also detected, albeit at lower significance. Fitting the line with a Gaussian gives a dispersion of  $\sigma_V = 99.9 \pm 14.7 \text{ km s}^{-1}$ , corresponding to a full width at half maximum (FWHM) of  $235 \pm 35 \text{ km s}^{-1}$ .

Figure 2 shows an image of the [C II] line and the underlying continuum emission. The map in the [C II] emission line (which was averaged from  $-153 \text{ km s}^{-1}$  to  $+102 \text{ km s}^{-1}$ ) results in a  $9.4\sigma$  detection at the near-infrared location of the quasar. The integrated flux of the line is  $1.03 \pm 0.14 \text{ Jy km s}^{-1}$  (or  $8.1 \pm 1.1 \times 10^{-21} \text{ W m}^{-2}$ ), which corresponds to a luminosity of  $L_{[\text{CII}]} = 1.2 \pm 0.2 \times 10^9 L_{\odot}$ . This [C II] luminosity is a factor of  $\sim 4$  lower than that of the bright  $z = 6.42$  quasar SDSS J1148+5251 ( $4.1 \pm 0.3 \times 10^9 L_{\odot}$ ; Maiolino et al. 2005; Walter et al. 2009). The width of the [C II] line of  $235 \pm 35 \text{ km s}^{-1}$  in J1120+0641 is, on the other hand, similar to the line width seen in SDSS J1148+5251 of  $350 \pm 50 \text{ km s}^{-1}$ .

The line free part of the spectrum can be used to estimate the far-infrared continuum emission around  $158 \mu\text{m}$  in the rest-frame of the quasar. Averaging the channels from  $-1500 \text{ km s}^{-1}$  to  $-290 \text{ km s}^{-1}$  and from  $+215 \text{ km s}^{-1}$  to  $+1500 \text{ km s}^{-1}$  results in a detection of the continuum at a level of  $0.61 \pm 0.16 \text{ mJy}$ . This is a factor  $\sim 2$  below the average  $250 \text{ GHz}$  flux density found towards all observed  $z \sim 6$  quasars<sup>2</sup> ( $1.26 \pm 0.10 \text{ mJy}$ ;

<sup>1</sup> <http://www.iram.fr/IRAMFR/GILDAS>

<sup>2</sup> Although the luminosity distance increases by  $\sim 20\%$  between  $z = 6$  and  $z = 7.1$ , the negative  $K$ -correction results in a flux density at a fixed observed frequency that is nearly constant. In our case, the observed continuum at  $235 \text{ GHz}$  will appear  $\sim 15\%$  brighter for a source at  $z = 7.1$  compared to one at  $z = 6$  observed at  $250 \text{ GHz}$  (assuming that the FIR emission comes from a grey

Wang et al. 2008), but comparable to the average flux density of  $z \sim 6$  quasars that were not individually detected at 1 mm ( $0.52 \pm 0.13$  mJy; Wang et al. 2008).

Finally, neither the [C II] emission line nor the underlying continuum are spatially resolved with the current resolution of the data, i.e.,  $2.02 \times 1.71$  arcsec<sup>2</sup>, corresponding to a spatial scale of  $10.4 \times 8.9$  kpc<sup>2</sup> at  $z \sim 7.1$ .

## 4. DISCUSSION

### 4.1. Far-infrared Luminosity

The far-infrared luminosity ( $L_{\text{FIR}}$ ) of J1120+0641 can be computed by approximating the shape of the far-infrared continuum with an optically thin graybody. Here we assume a dust temperature of  $T_d = 47$  K and dust emissivity power-law spectral index of  $\beta = 1.6$  ( $\kappa_\nu \propto \nu^\beta$ ), based on the mean spectral energy distribution (SED) of quasar hosts in the redshift range  $1.8 < z < 6.4$  (Beelen et al. 2006). The grey body is scaled to 0.61 mJy (our continuum detection) at a rest-frame frequency of  $\nu = 1900$  GHz. Following the prescription of Helou et al. (1988) and integrating the graybody from  $42.5$  to  $122.5$   $\mu\text{m}$  in the rest-frame, we derive for J1120+0641  $\log(L_{\text{FIR}}) = 12.15 \pm 0.12 L_\odot$ . Assuming a temperature of 41 K and a  $\beta = 1.95$  (the best-fitting values found for a sample of  $z = 4$  quasars, Priddey & McMahon 2001) gives a  $L_{\text{FIR}}$  that is 8% lower. If we instead fit our continuum detection to a template of Arp 220 or M82 (Silva et al. 1998), we derive a  $\log(L_{\text{FIR}}) = 11.90 \pm 0.12 L_\odot$  and  $\log(L_{\text{FIR}}) = 11.97 \pm 0.12 L_\odot$ , respectively. To conclude, our best estimate for  $L_{\text{FIR}}$  is in the range  $5.8 \times 10^{11} - 1.8 \times 10^{12} L_\odot$ .

From our detections of the FIR continuum we can estimate an SFR. A key question here is which fraction of the FIR emission in quasars is powered by star formation. Studies of lower redshift quasars found fractions ranging from 25% (e.g. Shi et al. 2007), >30%–100% (e.g. Schweitzer et al. 2006) to >50% (e.g. Walter et al. 2009). Below we assume that all the  $158 \mu\text{m}$  flux density arises from star formation. This should be treated as an upper limit on the SFR in J1120+0641.

Integrating the grey body from  $8 \mu\text{m}$  to  $1000 \mu\text{m}$  we get a total infrared luminosity of  $L_{\text{TIR}} = 2.0 \pm 0.5 \times 10^{12} L_\odot$ . Applying the relation between the total infrared luminosity and SFR by Kennicutt (1998), we derive an SFR of  $346 \pm 93 M_\odot \text{ yr}^{-1}$  adopting a Salpeter initial mass function (IMF). This SFR is a factor 1.51 lower when using a Kroupa IMF. On the other hand, using the template of Arp 220 (M82), we infer  $L_{\text{TIR}} = 1.3 \pm 0.3 \times 10^{12} L_\odot$  ( $L_{\text{TIR}} = 2.0 \pm 0.5 \times 10^{12} L_\odot$ ) and an SFR of  $219 \pm 59 M_\odot \text{ yr}^{-1}$  ( $340 \pm 91 M_\odot \text{ yr}^{-1}$ ).

The measured far-infrared flux density combined with the assumed dust temperature and emissivity can provide an estimate of the total dust mass  $M_{\text{dust}}$  in the quasar host (e.g., Hildebrand 1983; Magdis et al. 2011):

$$M_{\text{dust}} = \frac{f_{\nu, \text{cont}} D_L^2}{(1+z) \kappa_\lambda B_\nu(\lambda, T_d)}, \quad (1)$$

where  $f_{\nu, \text{cont}}$  is the far-infrared continuum flux density measured at rest-frame wavelength  $\lambda$ ,  $D_L$  is the luminosity distance,  $B_\nu(\lambda, T_d)$  is the Planck function at  $\lambda$  for

body with  $\beta = 1.6$ , see Section 4.1).

temperature  $T_d$ , and  $\kappa_\lambda$  is the dust mass opacity coefficient and is given by  $\kappa_\lambda = 0.77 (850 \mu\text{m}/\lambda)^\beta \text{ cm}^2 \text{ g}^{-1}$  (Dunne et al. 2000). Assuming that the properties of dust grains at  $z = 7$  are similar to those at low redshift, we derive  $M_{\text{dust}} = 9 \pm 2 \times 10^7 M_\odot$ , where the error only includes the uncertainty in the far-infrared continuum flux. Alternatively, we can make use of the templates of Arp 220 and M82 for which Silva et al. (1998) derived total dust masses. If the properties of the dust in J1120+0641 are similar to that in Arp 220 (M82), then we obtain a dust mass of  $1.3 \pm 0.3 \times 10^8 M_\odot$  ( $4.5 \pm 1.2 \times 10^8 M_\odot$ ).

### 4.2. [C II] Line to FIR Continuum Ratio

Surveys of local starbursts and quiescent star-forming galaxies have shown a tight correlation between  $L_{[\text{CII}]}$  and  $L_{\text{FIR}}$  (e.g., Stacey et al. 1991), although the ratio  $L_{[\text{CII}]} / L_{\text{FIR}}$  seems to decrease for galaxies with  $L_{\text{FIR}} > 10^{12} L_\odot$  (ULIRGs). In Figure 3 we plot a compilation of  $L_{[\text{CII}]} / L_{\text{FIR}}$  ratios as function of  $L_{\text{FIR}}$ , obtained from the literature. Also shown is the measurement of J1120+0641 of  $L_{[\text{CII}]} / L_{\text{FIR}} = 6.8 \times 10^{-4} - 2.1 \times 10^{-3}$ , based on our estimate of  $L_{\text{FIR}}$  of  $5.8 \times 10^{11} - 1.8 \times 10^{12} L_\odot$ . The ratio we measure for J1120+0641 is below those of local starburst galaxies and star-forming galaxies at  $z = 1 - 2$  which have  $L_{[\text{CII}]} / L_{\text{FIR}} \sim (3.1 \pm 0.5) \times 10^{-3}$ . However, it is a factor few higher than the only other  $L_{[\text{CII}]} / L_{\text{FIR}}$  ratio currently known above  $z > 6$ , the one measured in the  $z = 6.42$  quasar SDSS J1148+5251 (which has  $L_{[\text{CII}]} / L_{\text{FIR}} = 2.0 \pm 0.9 \times 10^{-4}$ ; Maiolino et al. 2005).

### 4.3. Dynamical Constraints

It is instructive to compare the implied gas dynamics to that of other high-redshift quasars. We here assume that the [C II] and CO line widths are roughly the same, which is the case for J1148+5251 at  $z = 6.42$  (Maiolino et al. 2005). The CO lines observed in  $z \sim 6$  quasars have line FWHMs between 160 and  $860 \text{ km s}^{-1}$ , with a median around  $350 \text{ km s}^{-1}$  (e.g. Wang et al. 2010, 2011). Quasars in the range  $1 < z < 5$  have a very similar median line width of  $\sim 325 \text{ km s}^{-1}$  (Solomon & Vanden Bout 2005; Riechers et al. 2006). The width of the [C II] line in J1120+0641 ( $235 \pm 35 \text{ km s}^{-1}$ ) is therefore less than the median found in  $z \sim 6$  quasars. Out of 12 published CO line widths in  $z \sim 6$  quasars only one has a line width less than  $235 \text{ km s}^{-1}$  (FWHM =  $160 \text{ km s}^{-1}$  in SDSS J1044-0125; Wang et al. 2010).

In the following discussion, we assume that the [C II] emission comes from a disk and that we can calculate a dynamical mass from the observed line width using  $M_{\text{dyn}} \sin^2 i \sim (\frac{3}{4} \text{FWHM})^2 R / G$  (Ho 2007), where  $R$  is the radius of the source and  $i$  its inclination angle. With an observed FWHM of  $235 \pm 35 \text{ km s}^{-1}$ , we derive a dynamical mass for J1120+0641 of  $M_{\text{dyn}} = (7.2 \pm 2.9) \times 10^9 (R/\text{kpc}) (\sin i)^{-2} M_\odot$ . Since our observations do not resolve the source spatially, we can only obtain an upper limit on the size of  $R \lesssim 5 \text{ kpc}$ . Assuming an (unknown) inclination angle of  $30^\circ$  leads to a dynamical mass of  $< 1.4 \times 10^{11} M_\odot$ . Even in the extreme case that all of this mass was present in the form of stars in the bulge of the

host galaxy and assuming that the bulge does not extend beyond 5 kpc, this would imply a black hole-bulge mass ratio of  $M_{\text{BH}}/M_{\text{bulge}} > 1.4_{-0.8}^{+1.2} \times 10^{-2}$ . Unless the inclination angle is below  $\sim 20^\circ$ , this is above the locally observed ratio of  $1.4 - 3.6 \times 10^{-3}$  (e.g., Merritt & Ferrarese 2001; Marconi & Hunt 2003; Graham 2012), similar to what has been found in other high-redshift quasars (Wang et al. 2008). Future observations, especially high resolution observations to derive the size and inclination angle of the emission with ALMA, will improve the constraints on the dynamical mass of the system and could lead to a better estimate of the  $M_{\text{BH}}/M_{\text{bulge}}$  ratio.

## 5. SUMMARY

Observations at 235 GHz using the PdBI resulted in the detection of the [C II] emission line and underlying dust continuum emission in the host galaxy of the quasar J1120+0641 at  $z = 7.085$ . These results show, for the first time, the existence of significant amounts of cold gas and dust at  $z > 7$ , when the universe was just 740 Myr old. Based on the mm observations, we can derive the following properties of the quasar host galaxy:

- The [C II] luminosity of  $1.2 \pm 0.2 \times 10^9 L_\odot$  is only a factor  $\sim 4$  lower than the one observed in the more luminous  $z = 6.42$  quasar J1148+5251. The width of the line ( $235 \pm 35 \text{ km s}^{-1}$ ) is smaller than what has typically been found in quasar host galaxies around  $z \sim 6$ . The emission remains unresolved at a resolution of  $2''.02 \times 1''.71$ , which corresponds to  $10.5 \times 8.9 \text{ kpc}^2$  at the redshift of the line.
- The far-infrared flux density (at a rest-frame wavelength of  $158 \mu\text{m}$ ) of  $0.61 \pm 0.16 \text{ mJy}$  implies, depending on the model that is used, a far-infrared luminosity of  $5.8 \times 10^{11} - 1.8 \times 10^{12} L_\odot$ . If all the far-infrared dust emission is powered by star formation, the SFR is between 160 and  $440 M_\odot \text{ yr}^{-1}$ . The total dust mass implied by the FIR emission is estimated to be in the range  $6.7 \times 10^7 - 5.7 \times 10^8 M_\odot$ . The  $L_{[\text{CII}]} / L_{\text{FIR}}$  ratio of  $6.8 \times 10^{-4} - 2.1 \times 10^{-3}$  is lower than those measured in local star-forming galaxies, but (at least) a factor  $\sim 3$  higher than in J1148+5251.
- If we assume that the [C II] emission arises from a disk geometry, then the narrow line width implies a relatively small dynamical mass of  $M_{\text{dyn}} = 7 \times 10^9 (R/\text{kpc}) (\sin i)^{-2} M_\odot$ . Taking an upper limit on the size of  $R < 5 \text{ kpc}$  results in a limit on the dynamical mass of  $M_{\text{dyn}} < 3.6 \times 10^{10} (\sin i)^{-2} M_\odot$ . Even if all of the dynamical mass is in the form of stars, the  $M_{\text{BH}}/M_{\text{bulge}}$  is above the locally observed ratio, unless the inclination angle is  $i < 20^\circ$ .

Future observations will allow us to better constrain the properties of the host galaxy of J1120+0641. For example, the detection of the far-infrared continuum at other frequencies with, e.g., ALMA or the upgraded PdBI, the Northern Extended Millimeter Array

(NOEMA), will constrain the shape of the FIR SED and thus  $L_{\text{FIR}}$ . On the other hand, observations of the [C II] line at higher spatial resolution will provide information about the extent of the line emission and will give better constraints on the dynamical mass. Finally, the detection of other (millimeter) emission lines such as CO, [C I]  $370 \mu\text{m}$ , [C I]  $230 \mu\text{m}$ , [O I]  $146 \mu\text{m}$  and/or [N II]  $122 \mu\text{m}$  (which could be observed with e.g. ALMA or NOEMA) will provide estimates of the total gas mass and could shed light on the metallicity and ionization state of the ISM in the host galaxy of J1120+0641.

We thank the referee for the constructive comments and suggestions, which improved the manuscript. Based on observations carried out with the IRAM Plateau de Bure Interferometer. IRAM is supported by INSU/CNRS (France), MPG (Germany), and IGN (Spain).

*Facility:* IRAM:Interferometer.

## REFERENCES

- Beelen, A., Cox, P., Benford, D. J., et al. 2006, ApJ, 642, 694  
 Cox, P., Krips, M., Neri, R., et al. 2011, ApJ, 740, 63  
 De Breuck, C., Maiolino, R., Caselli, P., et al. 2011, A&A, 530, L8  
 Dunne, L., Eales, S., Edmunds, M., et al. 2000, MNRAS, 315, 115  
 Graham, A. W. 2012, ApJ, 746, 113  
 Helou, G., Khan, I. R., Malek, L., & Boehmer, L. 1988, ApJS, 68, 151  
 Hewett, P. C. & Wild, V. 2010, MNRAS, 405, 2302  
 Hildebrand, R. H. 1983, QJRAS, 24, 267  
 Ho, L. C. 2007, ApJ, 669, 821  
 Isaak, K. G., McMahon, R. G., Hills, R. E., & Withington, S. 1994, MNRAS, 269, L28  
 Ivison, R. J., Swinbank, A. M., Swinyard, B., et al. 2010, A&A, 518, L35  
 Kennicutt, R. C. 1998, ARA&A, 36, 189  
 Magdis, G. E., Daddi, E., Elbaz, D., et al. 2011, ApJ, 740, L15  
 Maiolino, R., Caselli, P., Nagao, T., et al. 2009, A&A, 500, L1  
 Maiolino, R., Cox, P., Caselli, P., et al. 2005, A&A, 440, L51  
 Malhotra, S., Kaufman, M. J., Hollenbach, D., et al. 2001, ApJ, 561, 766  
 Marconi, A. & Hunt, L. K. 2003, ApJ, 589, L21  
 Merritt, D. & Ferrarese, L. 2001, MNRAS, 320, L30  
 Mortlock, D. J., Warren, S. J., Venemans, B. P., et al. 2011, Nature, 474, 616  
 Priddey, R. S. & McMahon, R. G. 2001, MNRAS, 324, L17  
 Riechers, D. A., Walter, F., Carilli, C. L., et al. 2006, ApJ, 650, 604  
 Schweitzer, M., Lutz, D., Sturm, E., et al. 2006, ApJ, 649, 79  
 Shi, Y., Ogle, P., Rieke, G. H., et al. 2007, ApJ, 669, 841  
 Silva, L., Granato, G. L., Bressan, A., & Danese, L. 1998, ApJ, 509, 103  
 Solomon, P. M. & Vanden Bout, P. A. 2005, ARA&A, 43, 677  
 Stacey, G. J., Geis, N., Genzel, R., et al. 1991, ApJ, 373, 423  
 Stacey, G. J., Hailey-Dunsheath, S., Ferkinhoff, C., et al. 2010, ApJ, 724, 957  
 Tremaine, S., Gebhardt, K., Bender, R., et al. 2002, ApJ, 574, 740  
 Wagg, J., Carilli, C. L., Wilner, D. J., et al. 2010, A&A, 519, L1  
 Walter, F., Riechers, D., Cox, P., et al. 2009, Nature, 457, 699  
 Wang, R., Carilli, C. L., Neri, R., et al. 2010, ApJ, 714, 699  
 Wang, R., Carilli, C. L., Wagg, J., et al. 2008, ApJ, 687, 848  
 Wang, R., Wagg, J., Carilli, C. L., et al. 2011, ApJ, 739, L34  
 Wright, E. L., Mather, J. C., Bennett, C. L., et al. 1991, ApJ, 381, 200

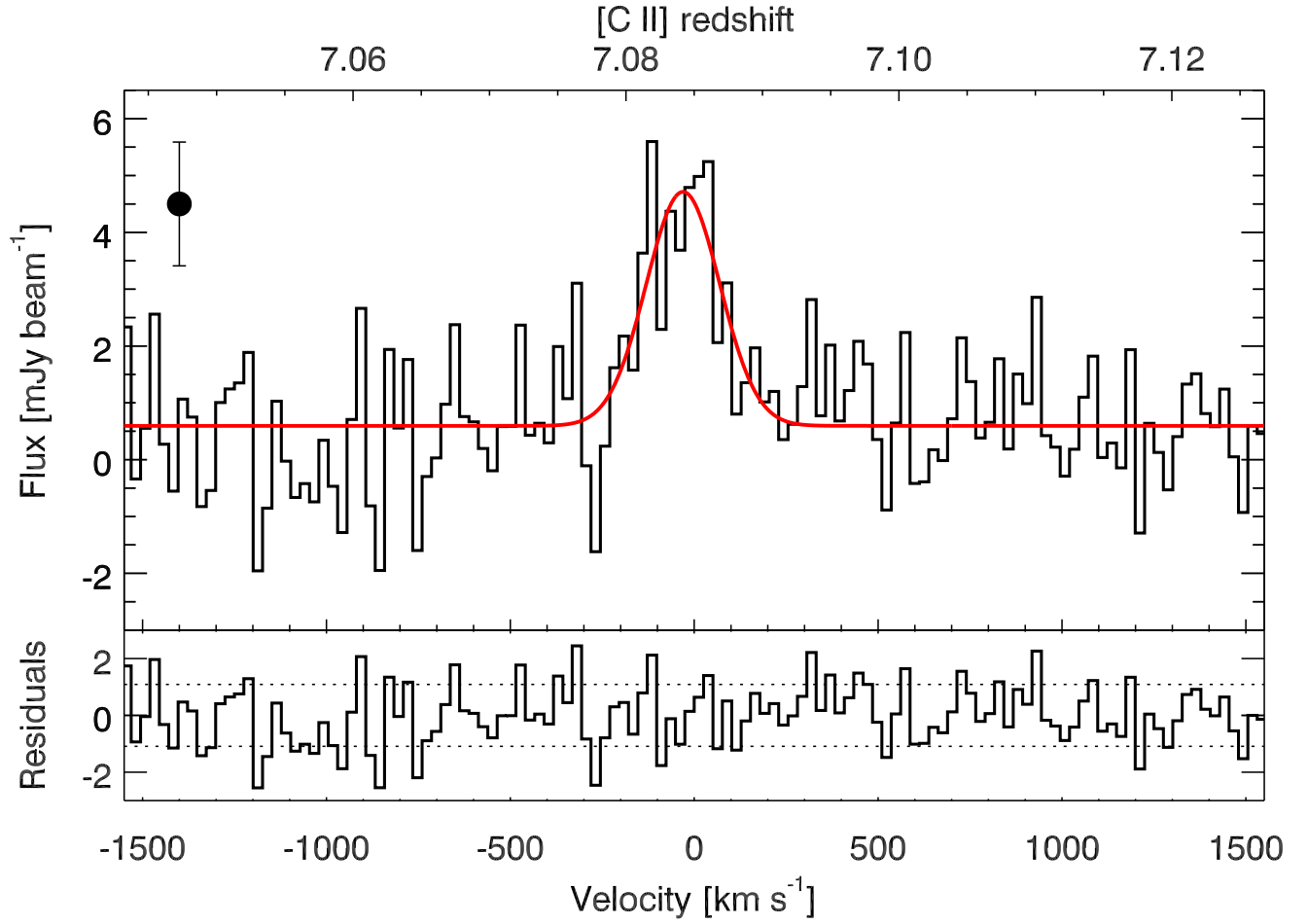


**Figure 1.** Plateau de Bure Interferometer spectrum of J1120+0641 of the redshifted [C II]  $158\ \mu\text{m}$  line. The channels have a width of 20 MHz ( $\sim 25\ \text{km s}^{-1}$ ). The noise per bin is  $1.09\ \text{mJy beam}^{-1}$  and is shown in the upper-left corner. The published redshift of  $z = 7.085$  (derived from rest-frame UV lines of the quasar; Mortlock et al. 2011) has been taken as the zero point of the velocity scale. The red, solid curve is a Gaussian fit to the spectrum and shows that faint continuum emission is also detected in the quasar host. The residuals of the fit are plotted below the spectrum. The dotted lines represent  $+\sigma$  and  $-\sigma$ , with  $\sigma$  the noise per bin of  $1.09\ \text{mJy beam}^{-1}$ .

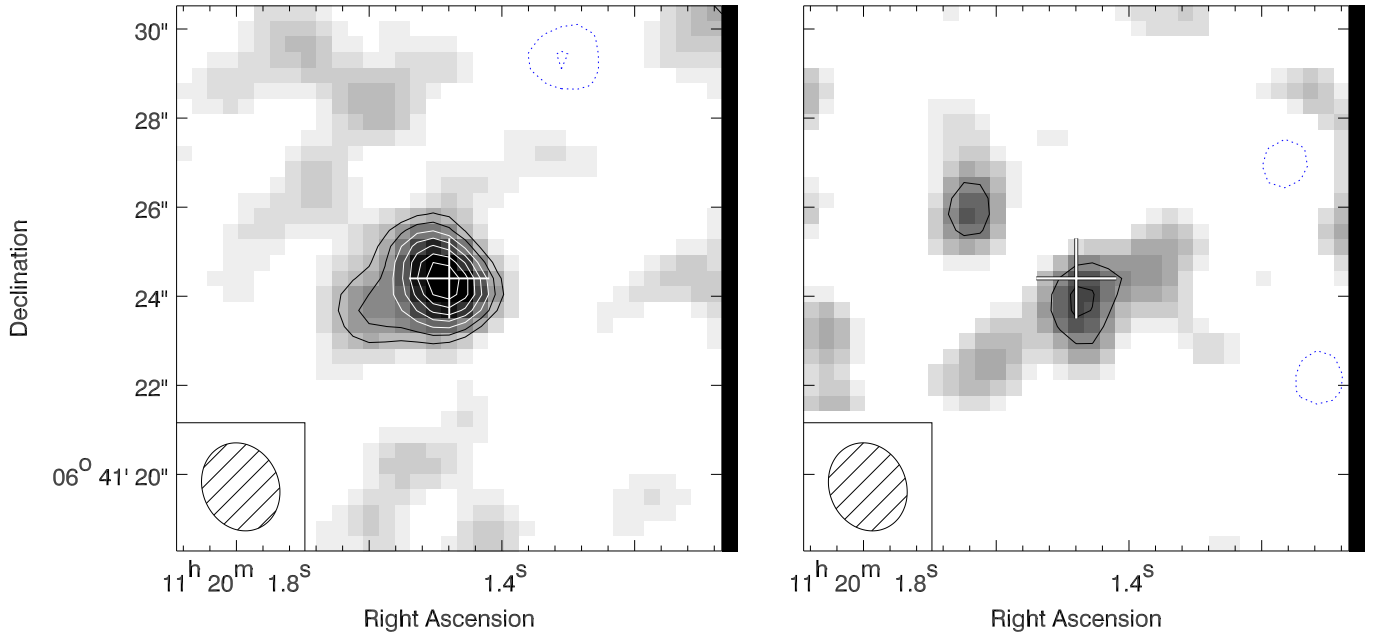


**Figure 2.** Left: image showing the a map constructed from the averaged emission between  $-153$  and  $+102$   $\text{km s}^{-1}$ . The contours are  $-3.5\sigma$ ,  $-2.5\sigma$  (blue, dotted lines),  $2.5\sigma$ ,  $3.5\sigma$  (black, solid lines),  $4.5\sigma$ ,  $5.5\sigma$ ,  $6.5\sigma$ ,  $7.5\sigma$  and  $8.5\sigma$  (white, solid lines), with  $\sigma$  the rms noise of  $0.43$   $\text{mJy beam}^{-1}$ . The cross indicates the near-infrared location of the quasar. The beam ( $2.02 \times 1.71$   $\text{arcsec}^2$ ) is overplotted at the bottom left corner of the image – the emission is unresolved at this resolution. Right: map of the underlying rest-frame FIR continuum based on the line-free channels with the same spacing in sigma. The rms noise in this map is  $0.16$   $\text{mJy beam}^{-1}$ .

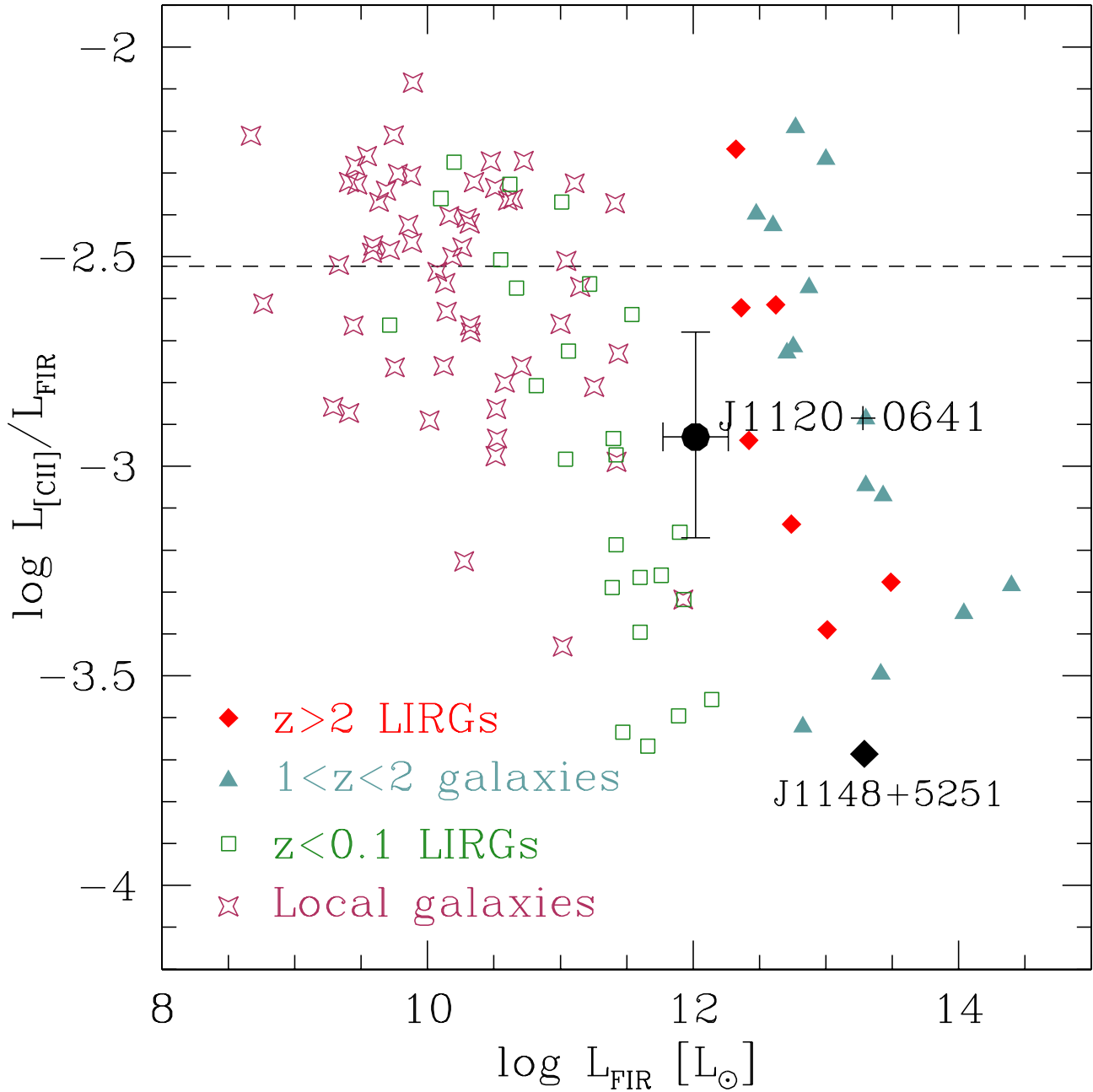


**Figure 3.** Ratio of [C II] luminosity over FIR luminosity as function of FIR luminosity. The values derived for ULAS J1120+0641 are indicated with the filled circle. Also plotted are values for local galaxies (open stars; Malhotra et al. 2001), low redshift luminous infrared galaxies (LIRGs, open squares; Maiolino et al. 2009), galaxies at  $1 < z < 2$  (filled triangles; Stacey et al. 2010) and  $z > 2$  LIRGs (filled diamonds; Maiolino et al. 2009; Ivison et al. 2010; Wagg et al. 2010; De Breuck et al. 2011; Cox et al. 2011). The  $L_{\text{[CII]}}/L_{\text{FIR}}$  ratio found for J1120+0641 is roughly between the average ratio found for local star-forming galaxies (dashed line) and that of the  $z = 6.4$  quasar J1148+5251 (large, black diamond).